

## Hysteretic behaviour of high strength S690 steel materials under low cycle high strain tests

<sup>2</sup>Ho, H.C., <sup>1,2</sup>Liu, X., <sup>1,2</sup>Chung K.F., <sup>3</sup>Elghazouli, A.Y. and <sup>1</sup>Xiao, M.

<sup>1</sup>Department of Civil and Environmental Engineering,

The Hong Kong Polytechnic University, Hong Kong SAR, China.

<sup>2</sup>Chinese National Engineering Research Centre for Steel Construction (Hong Kong Branch),  
The Hong Kong Polytechnic University, Hong Kong SAR, China.

<sup>3</sup>Department of Civil and Environmental Engineering, Imperial College London, U.K.

### Abstract

Ductility requirements on steel materials are conventionally derived from monotonic tests, and they represent important criteria in selecting suitable steel materials in structural applications. In general, there is no additional requirements stipulated for quantifying these steel materials to be used in seismic resistant structures. As structural responses of steel materials under cyclic loads are rather different from those under monotonic actions, it is important to establish new ductility requirements based on cyclic tests, especially for high strength steel materials such as S690 to be quantified for use in seismic resistant structures.

In this paper, a detailed experimental investigation into the structural behaviour of S690 steel coupons under both monotonic and cyclic actions has been described. A total of 6 monotonic tensile tests were conducted to establish basic mechanical properties of the S690 steel materials. Moreover, 36 cyclic tests were conducted in order to investigate the hysteretic behaviour of the S690 steel materials under various target strains and loading frequencies.

Based on test results obtained from monotonic tensile tests, all coupons of S690 steel plates tested in the experimental investigation were found to be able to satisfy current ductility requirements stipulated in EN 1993-1-1 and EN 1993-1-12. Moreover, many coupons were shown to be able to complete 20 cycles in the proposed cyclic tests with target strains  $\epsilon_m$  at  $\pm 2.5\%$ ,  $\pm 5.0\%$ ,  $\pm 7.5\%$ , and  $\pm 10.0\%$  under various loading frequencies  $f = 0.1, 0.5, 1.0$  and  $2.0$  Hz. However, some coupons fractured at the 20<sup>th</sup> cycle when the target strains were  $\pm 10.0\%$  irrespective of the loading frequencies. As significant change occurs in cross-sectional areas of the coupons, it is important to use instantaneous diameters to evaluate true stresses which result in symmetric hysteretic curves. Furthermore, owing to strain hardening, significant strength enhancement was found and quantified in these cyclic tests, depending on magnitudes of the target strains. Detailed hysteretic behaviour characterised in this investigation can be directly employed to develop reliable constitutive models of high strength S690 materials under seismic loading conditions.

### Keywords:

High strength steel materials; hysteretic behaviour; ductility; monotonic tests; cyclic tests.

## 1. Introduction

Over the past twenty years, various grades of high strength steel materials, such as S690, S890, and S960 have been produced successfully in many parts of the world, and they are highly attractive to structural engineers because of their high strength to weight ratios. These steel materials offer excellent mechanical properties, such as yield and tensile strengths as well as toughness, in comparison with normal strength steel materials. Wider adoption of high strength steel materials would lead to a significant reduction in sizes of structural members as well as self-weights of building structures with improved constructability, leading to savings in overall construction time and costs.

According to modern structural design standards, such as EN 1993-1-1, various ductility requirements for S235 to S460 steel materials, which are quantified according to mechanical properties derived primarily from monotonic tests, are stipulated as follows:

i) tensile to yield strength ratio,  $f_u / f_y \geq 1.10$ , (1a)

ii) strain at fracture,  $\epsilon_L \geq 15 \%$ , and (1b)

iii) strain corresponding to tensile strength,  $\epsilon_u \geq 15 f_y / E_s$ . (1c)

For S690 steel materials, the minimum value of  $f_u / f_y$  is revised to 1.05 while the value of  $\epsilon_L$  is re-defined to be  $\geq 10 \%$  according to EN 1993-1-12. It should be noted that currently, no additional ductility requirements on steel materials are specifically stipulated for applications in seismic resistant structures.

As the structural behaviour of steel materials under cyclic loads is different from that under monotonic tests, it is important to establish new ductility requirements based on cyclic tests on steel materials, especially for high strength steel materials, such as S690, to be qualified to be used in seismic resistant structures.

In the recent years, a number of studies reported cyclic tests on specifically designed coupons of various types of steel materials to examine their hysteretic characteristics. These cyclic tests were typically conducted according to idealized pre-defined displacement histories. It should be noted that many researchers (Fournier *et al.* 2006 a & b, Nip *et al.* 2010, Khan *et al.* 2012, Li *et al.* 2013, Chen *et al.* 2013 and Zhou *et al.* 2015) conducted experimental investigations to examine hysteretic behaviour of structural steel materials with different testing methods reflecting different applications and experimental constraints. Researchers in fatigue engineering (Fournier *et al.* 2006 a & b, Khan *et al.* 2012, and Li *et al.* 2013) focused on fracture mechanisms as well as microstructures of the steel materials at various temperatures, while researchers in structural engineering (Nip *et al.* 2010, Chen *et al.* 2013 and Zhou *et al.* 2015) examined structural behaviour of the steel materials under different loading protocols and strain amplitudes.

In order to identify suitable testing methods for cyclic tests on steel materials to be quantified for use in seismic design, three commonly adopted testing methods are compared:

i) *Recommendations for assessing behaviour of structural steel elements under cyclic loads (ECCS, 1986)*

This early ECCS Recommendations gave recommendations in standardizing a cyclic test method to facilitate comparison on structural behaviour against various structural elements under cyclic actions. In general, a loading protocol is defined through i) a conventional limit of elastic range designated as  $F_y$ , and ii) corresponding deformation obtained from monotonic tests in both tension and compression actions, or sagging and hogging actions, designated as  $\epsilon_y$ , as shown in Figure 1a). However, there is little technical information provided on: i) choice and use of the loading protocol, ii) relationship between structural response under seismic action and cyclic ductility under different levels of seismicity.

ii) *FEMA-461: Interim testing protocols for determining the seismic performance characteristics of structural and non-structural components (2007)*

Since its publication in 2007, FEMA-461 has been regarded by many researchers as the

definitive guidance document on selection of the loading protocols, and a stepwise loading protocol, as shown in Figure 1b), was recommended in cyclic tests to investigate hysteretic behaviour of steel materials.

iii) AISC 341: *Seismic Provisions for Structural Steel Buildings (2016)*

In general, AISC 341 focuses on the seismic design of steel and composite structures. It provides a loading protocol for cyclic tests, as shown in Figure 1c), which is suitable for qualification of beam-to-column connections. A comparison with the protocol given in FEMA shows that the total number of cycles is increased from 20 to 30 in achieving the same value of the target strain while the step factor is decreased accordingly.

Experimental investigations on the hysteretic behaviour of various types of carbon steel and stainless steel materials have also used different loading protocols, namely: i) cyclic ascend loading protocol, ii) cyclic alternate loading protocol, and iii) cyclic tensile loading protocol at a maximum strain amplitude of  $\pm 2\%$  (Chen *et al.* 2013, and Zhou *et al.* 2015).

Consequently, it is highly desirable to establish a standardized testing method to define a suitable loading protocol, a test specimen of suitable geometry, and an appropriate loading frequency for characterization of high strength S690 steel materials to be qualified for use in seismic design.

In this investigation, a detailed experimental investigation into structural behaviour of S690 steel materials under both monotonic and cyclic actions as follows:

- i) 6 monotonic tensile tests on standardized cylindrical coupons of S690 steel materials were conducted, and deformations were measured with strain gauges at small deformations, and with measurements on digital photos at large deformations; and
- ii) a total of 36 cyclic tests on funnel-shaped cylindrical coupons of S690 steel materials were also conducted, and cyclic responses were measured with a high precision extensometer at both small and large deformations.

The specific objectives of the current investigation include detailed examination of the

following:

- a) mechanical properties of S690 steel materials, in particular, their ductility at large deformations under monotonic actions;
- b) hysteretic behaviour of S690 steel materials at large deformations under cyclic actions of practical ranges of axial strains, loading frequencies, and straining rates; and
- c) instantaneous diameters, and hence, reduced cross-sections of coupons at large deformations.

Table 1 summarizes typical chemical compositions of S690 steel plates used in this study together with requirements on chemical compositions of S690 steel materials given in EN 10025-6. All chemical compositions of the steel plates are within the maximum limits, especially for P and S, which have serious adverse effects on mechanical properties of the steel plates. There are two different types of test coupons, namely, i) a standardized cylindrical coupon, and ii) a funnel-shaped coupon, according to various material testing standards for cyclic tests, such as BS 3518-3 (1963), GB/T 15248 (1994), and ISO 12106 (2003). In general, the cylindrical coupon is considered to be suitable for cyclic tests at a maximum strain of up to 2% while the funnel-shaped coupon is considered to be suitable for cyclic tests up to a maximum strain of 15%. Moreover, for those cylindrical test coupons, the gauge length,  $l_g$ , is recommended to be  $1d$  to  $3d$  where  $d$  is the diameter of the coupon within its gauge length. However, there is no specific recommendation to the gauge length of those funnel-shaped coupons, which can result in inconsistency between various cyclic tests due to different types of test coupons and gauge lengths.

## **2. Monotonic Tensile Tests**

As shown in Table 2, a total of 6 standardized cylindrical coupons were tested in the monotonic tensile tests. It should be noted that Coupons T690-A1/2/3 were cut from a 16 mm thick S690 steel plate while Coupons T690-B1/2/3 were cut from another S690 steel plate. Detailed dimensions of the test coupons are shown in Figure 2, and their diameter,  $d$ , is 6mm while their gauge length,  $l_g$ , is 30mm. The relationships between the diameters and the gauge lengths of the cylindrical coupons comply with requirements in BS EN 6892-1 (CEN, 2009). All the test coupons were sampled from appropriate locations of parent steel plates, and machined into dimensions using a high-precision Computer Numerical Control (CNC) system.

## 2.1 Test set-up, instrumentation and procedures

A high-precision test machine, namely, Testometric CX M500 Testing Machine, was employed to conduct these tensile tests, as shown in Figure 3. In each test, two strain gauges were attached firmly to the centre of the coupon to acquire deformations of the coupon during the initial loading stage of the test, that is, up to yielding of the coupon. A high resolution camera was also mounted in front of the coupon in the commencement of the test, and digital images of the coupon were taken at regular intervals to acquire deformations of the coupon throughout the test. It should be noted that the 30 mm long gauge length of the coupon was equally divided into six segments to facilitate measurements in the digital images.

## 2.2 Test results

All the monotonic tensile tests were conducted successfully, and Figure 4 plots all the stress-strain curves of high strength S690 steel materials onto the same graph for direct comparison. In general, before necking occurred in the coupons, deformations along parallel portions of the coupons were assumed to be fairly uniform (Ling, 1996; Roylance, 2001), and data measured from strain gauges were readily adopted as the average strains within the gauge length of the coupons.

It should be noted that the loading rates in the tests were carefully controlled at various stages, and Table 3 summarizes these loading rates together with recommended values given in BS EN ISO 6892-1. As shown in Figures 5 and 6, the monotonic tests were divided into three different phases, namely i) Phase 1 for determination of the Young's modulus,  $E_s$ , ii) Phase 2 for determination of the yield strength,  $f_y$ , and, iii) Phase 3 for determination of the tensile strength,  $f_u$ , and the elongation at fracture,  $\epsilon_L$ , respectively. As shown in Table 3, these loading rates adopted in the tests were sufficiently small to obtain accurate values of the mechanical properties of the coupons. Hence, after data analyses, various material properties of these S690 steel materials are attained and summarized in Table 4. As the coefficients of variations of these material properties are very small, the test results are considered to be highly

consistent. Hence, the average yield strength,  $f_y$ , of the coupons is found to be 801 N/mm<sup>2</sup> while their average tensile strength,  $f_u$ , is 853 N/mm<sup>2</sup>. Thus, the average tensile to yield strength ratio,  $f_u / f_y$  is found to be 1.05. It should be noted that for all the coupons, the elongations at fracture,  $\epsilon_L$ , are found to be larger than 15% while the strains corresponding to tensile strengths,  $\epsilon_u$  are larger than  $15 f_y / E_s$ . Consequently, all the coupons meet all ductility requirements specified in EN 1993-1-12.

As mentioned above, a high resolution camera was mounted in front of the coupon, and digital images of the coupon were taken to acquire their deformations throughout the entire tests. With a fixed focal distance throughout a test, the dimensions of the coupon are directly proportional to the number of pixels appearing in the images. Hence, deformations of the coupons, such as changes in their gauge lengths under different load or deformation levels are readily obtained from counting the number of pixels of corresponding images of the deformed coupons. Table 5 illustrates a typical example to determine deformed (or elongated) gauge lengths, and hence, corresponding strains of a coupon under various deformation levels in a monotonic tensile test.

Figure 7 plots typical strain variations of all the six segments within the gauge length of a coupon under different deformation conditions. It is apparent that while the strains of all the segments are fairly uniform at both the yield and the ultimate conditions, there is a highly localized strain in Segment 4 at fracture. Table 6 presents typical measured strains of various segments within the gauge length of a coupon under various deformation conditions. It is shown that:

- i) under yield condition, the strains are shown to vary with the range of 0.4 to 0.9 %;
- ii) under ultimate condition, the strains are shown to be rather non-uniform as the maximum strain among all of the segments is 8.1 % while the average strain of the six segments is merely 6.7 %; and
- iii) under fracture condition, the average strain of the six segments is shown to be 17.6 % while the maximum strain among all of the segments is found to be 62.5 % as a highly localized necking occurs in Segment 4 only.

It should be noted that owing to the set-up of this measurement method, accuracy of measurements under yield condition in the coupons are rather low as the deformations are small. Hence, readings from strain gauges under yield condition should be used instead. For measurements under ultimate and fracture conditions, accurate measurements are obtained.

Based on the research work by Ho et al. (2017), various classical transformation rules from engineering stress-strain ( $\sigma - \epsilon$ ) curves into true stress strain ( $\sigma_t - \epsilon$ ) curves are only applicable up to a deformation at about 5%. For larger deformations, say 10%, or even up to fracture, instantaneous diameters of test coupons, and hence, their instantaneous cross-sectional areas, should be used in order to obtain true stresses,  $\sigma_t$ , accurately. In order to assess and compare the hysteretic behaviour of various S690 steel materials, true stresses are normalized with their respective yield strengths to give a true stress ratio,  $\beta_t$ , as follows:

$$\beta_t = \sigma_t / f_{0.2,c} \quad (2)$$

where  $f_{0.2,c}$  is the 0.2% proof strength under cyclic loads. Figure 8 plots all the normalized true stress ratio engineering strain ( $\beta_t - \epsilon$ ) curves of the S690 steel materials onto the same graph for direct comparison.

### 3. Low Cycle High Strain Cyclic Tests

A total of 36 funnel-shaped cylindrical coupons were tested in low cycle high strain cyclic tests. In Series A, there were 20 coupons which were cut from the 16 mm thick S690 steel plate while in Series B, there were another 20 coupons which were cut from the 20 mm thick S690 steel plate. Detailed dimensions of the coupons are shown in Figure 9, and the diameter,  $d$ , and the gauge length,  $l_g$ , of the coupons are 5 mm and 10 mm respectively. All the dimensions of these coupons comply with requirements in BS 3518-3 (1963). It should be noted that these funnel-shaped cylindrical coupons are employed in order to prevent occurrence of plastic buckling of the coupons during testing as the strain demand in these tests well exceeds 2%. All the test coupons were sampled from appropriate locations of parent steel plates, and cut and milled using a high-precision Computer Numerical Control (CNC) system.

In order to establish deformation characteristics of various steel materials for possible application in seismic resistant structures, the loading protocol given in FEMA-461 (2007) is adopted together with the following parameters in the cyclic tests for its wide application in engineering design and research purposes:



a) Target strains

In general, the strain demand for different structural forms should be determined with a detailed structural analysis according to a specific seismicity or a level of seismic loads under consideration. According to strain demands in typical steel structures under high seismicity, the maximum strain demand (Shafei & Zareian 2008, and Tsitos & Elghazouli 2017) may reach 18 times of the yield strain,  $\epsilon_y$  of the steel material, which was estimated to be 2.5 %. Moreover, previous experimental investigations on low cyclic high strain cyclic tests of stainless steel materials were conducted with different strain amplitudes at  $\pm 1\%$ ,  $\pm 4\%$  and  $\pm 7\%$  (Nip *et al.* 2010).

Consequently, in the absence of a detailed structural analysis and to cater for application to a wide range of structural configurations, four different values of target strain,  $\epsilon_m$ , are proposed, namely, i)  $\pm 2.5\%$ , ii)  $\pm 5.0\%$ , iii)  $\pm 7.5\%$  and iv)  $\pm 10.0\%$ , to investigate the hysteretic behaviour of the S690 steel materials under various deformation requirements. The strain amplitudes for various load cycles of the adopted loading protocol according to FEMA-461 (2007) for a target strain  $\epsilon_m$  at  $\pm 10.0\%$  are summarized in Table 7. It should be noted that the magnitude of the first strain imposed is 0.48% which is larger than the yielding strain. Hence, plastic hardening is readily developed in the coupons after the first hysteretic loop is applied.

b) Loading frequency

Different testing standards give different recommendations on the loading rates of the cyclic tests. At present, there is no standardized loading rate of cyclic tests for seismic engineering. After considering recommendations given in FEMA-461 (2007) and displacement responses of SDOF systems (Mergos and Beyer, 2014), the acceptable loading frequency is proposed to range from 0.01 Hz to 10 Hz, for low straining rates under seismic actions. For practical application in seismic engineering, the following loading frequencies are proposed in the present investigation:  $f = 0.1, 0.5, 1.0$  and  $2.0$  Hz. The maximum straining rates at various load cycles of the adopted loading protocol according to FEMA-461 (2007) for a target strain  $\epsilon_m = \pm 10.0\%$  and a frequency  $f = 0.1$  Hz are summarized in Table 7.

The test programme of cyclic tests is summarized in Table 8:

- Test Series A

There are two sub-series under Test Series A. In Test Series A1, a total of four target strains,  $\epsilon_m$ , are adopted, i.e.  $\epsilon_m = \pm 2.5\%$ ,  $\pm 5.0\%$ ,  $\pm 7.5\%$  and  $\pm 10.0\%$  while the loading frequency,  $f$ , is kept to be 0.1 Hz in all tests. In Test Series A2, a total of two target strains  $\epsilon_m$ , namely,  $\pm 5.0$  and  $\pm 10.0\%$  are adopted while three different loading frequencies,  $f$ , are adopted, i.e.  $f = 0.5$ , 1.0 and 2.0 Hz. Hence, the hysteretic behaviour of the coupons is tested at a wide range of target strains under a constant loading frequency.

- Test Series B

In this Test Series, a total of two target strains,  $\epsilon_m$ , are adopted, i.e.  $\epsilon_m = \pm 5.0$  and  $\pm 10.0\%$  while four different loading frequencies,  $f$ , are adopted, i.e.  $f = 0.1$ , 0.5, 1.0 and 2.0 Hz. Hence, the hysteretic behaviour of the coupons is tested at a wide range of target strains and loading frequencies same as those in Test Series A in order to facilitate direct comparison among test results in both Test Series.

It should be noted that for each combination of target strains and loading frequency, two coupons were tested to allow comparison of test data.

### 3.1 Test set-up, instrumentation and procedures

An advanced MTS-810 Material Test System was employed to carry out these cyclic tests, and a matching MTS 632.13F-20 Extensometer was employed to acquire instantaneous deformations at regular time intervals with a high frequency data acquisition system. Figure 10 illustrates typical set-up of the cyclic tests together with a typical fractured coupon.

### 3.2 Test results

Figure 11 shows hysteretic curves of Series A1 with four different target strains  $\epsilon_m$  under a loading frequency,  $f = 0.1$  Hz while Figure 12 depicts typical results of cyclic tests with two different target strains  $\epsilon_m$  at  $\pm 5$  and  $\pm 10\%$  under four loading frequencies. It is shown that in

all tests, effective hysteretic loops are achieved, indicating good energy dissipation capacity under practical ranges of seismic actions. As the hysteretic curves of Series B are found to be very similar to those shown in Figures 11 and 12, for brevity, they are not presented herein.

Table 9 summaries key parameters in defining hysteretic behaviour of the coupons in both Test Series A and B, including 0.2% proof strengths  $f_{0.2,c}$ , strengths at target strain  $f_{\epsilon_m,c}$ , numbers of cycles completed before fracture, and strength enhancement factors  $\eta$ . Discrepancies between two repeated tests are found to be typically smaller than 2%. It should be noted that:

- All the cyclic tests in Test Series A1 with a target strain  $\epsilon_m$  at  $\pm 2.5$ ,  $\pm 5.0$ , and  $7.5\%$  have completed all the 20 loading cycles when the loading frequency is 0.1 Hz. For those cyclic tests in Test Series A1 with a target strain  $\epsilon_m$  at  $\pm 10.0\%$  and  $f = 0.1$  Hz, they have completed 19 cycles successfully, but fracture occur in these test coupons during the 20<sup>th</sup> loading cycle.
- For tests in Test Series A2 with  $f = 0.1, 0.5, 1.0$  and  $2.0$  Hz, all the tests completed all the 20 loading cycles at a target strain at  $\pm 5.0\%$ , but only 19 loading cycles at a target strain at  $\pm 10.0\%$ .
- All the cyclic tests in Test Series B1 with a target strain  $\epsilon_m$  at  $\pm 2.5$ ,  $\pm 5.0$ ,  $\pm 7.5$  and  $\pm 10.0\%$  have completed all the 20 loading cycles when the loading frequency is 0.1 Hz.
- All the cyclic tests in Test Series B2 with  $f = 0.1, 0.5, 1.0$  and  $2.0$  Hz, have completed all the 20 loading cycles at a target strain at  $\pm 5.0$  and  $\pm 10.0\%$ .
- The engineering stresses at target strains in compression and in tension are significantly different, and the hysteretic curves are unsymmetrical.

In summary, all the coupons perform well under low cycle high strain cyclic tests, with a maximum strain amplitude up to  $\pm 10\%$ . Moreover, the loading frequencies have little impact on the hysteretic behaviour of the S690 steel materials, provided that the loading frequencies vary within the range of 0.1 to 2.0 Hz.

### 3.2.1 Strength enhancement factor

For direct comparison, all hysteretic loops of various cyclic tests under different target strains

are plotted together with monotonic engineering stress strain curve in Figure 13. This shows the extent of cyclic hardening or softening taken place in the coupons under cyclic tests.

Moreover, backbone curves from these cyclic tests are derived according to the recommendations of the NERHRP Seismic Design Brief 2010 (Deierlein et al. 2010), and the Guidelines for Performance-Based Seismic Design for Tall Buildings (PEER, 2010). In order to facilitate direct comparison, a Strength Enhancement Factor,  $\eta$ , is established to quantify hysteretic behaviour of the test coupons as follows:

$$\eta = f_{\varepsilon_m, c} / f_{0.2, c} \quad (3)$$

where  $f_{\varepsilon_m, c}$  is the strength at a strain demand,  $\varepsilon_m$ , under cyclic loads; and  $f_{0.2, c}$  is the 0.2% proof strength under cyclic loads;

As shown in Figure 14, the Strength Enhancement Factor,  $\eta$ , describes any enhancement on the yield strength of a test coupon at a specific strain demand  $\varepsilon_m$  over the basic yield strength of the steel material under cyclic condition in different backbone curves. All the engineering stresses at respective target strains of cyclic tests in Test Series A and B are presented in Table 9, and strength enhancement factors are also provided for direct comparison. It is shown that all these Strength Enhancement Factors for cyclic tests in Test Series A and B under compression differ significantly from those under tension, especially for those curves with large target strains.

### 3.2.2 Instantaneous diameters

In order to investigate reasons of asymmetry in these hysteretic curves, digital images of these coupons were utilized to measure instantaneous diameters of a typical coupon during tests. Based on various measurements shown in Figure 15, Figure 16 plots measured values of the instantaneous diameters,  $d_i$ , of the coupon under various strain amplitudes. It is shown that the coupons exhibit necking with a considerable reduction in diameter under tension. The instantaneous diameters are found to increase in magnitude under small compression, but reduced in magnitude under large compression. Hence, a general formula is proposed to estimate the instantaneous diameters ( $d_i$ ) under different strain amplitudes ( $\varepsilon$ ) as follows:

$$d_i = -0.0087\varepsilon^2 - 0.043\varepsilon + 4.95 \quad (4)$$

Figure 17 plots the value of  $d^2 / d_i^2$  against different values of strain,  $\varepsilon$ , as correction factors applied to the engineering stresses,  $\sigma$ , to determine the values of true stresses,  $\sigma_t$ .

### 3.2.3 True-stress engineering strain hysteretic behaviour

Based on the proposed formula of measured instantaneous diameters, true-stress engineering strain ( $\sigma_t - \varepsilon$ ) hysteretic curves are obtained for those cyclic tests in Test Series A, and results under various target strains are plotted in Figures 18 and 19. It is evident that only small discrepancies exist between true compressive stresses and true tensile stresses at different strains. Hence, asymmetry is successfully eliminated to a large extent in these backbone curves after replacing engineering stresses,  $\sigma$ , with true stresses,  $\sigma_t$ .

Moreover, Table 10 summaries the key results of true stress engineering strain ( $\sigma_t - \varepsilon$ ) hysteretic behaviour, including 0.2% proof strength  $f_{0.2,c}$ , strength at target strain  $f_{\varepsilon m,c}$ , number of cycles completed and strength enhancement factor  $f_{\varepsilon m,c} / f_{0.2,c}$  for cyclic tests in Test Series A and B. It is found that for all the coupons in Test Series A and B under different target strains and loading frequencies:

- the strengths at target compressive strains are very close to those at target tensile strains, and
- the corresponding strength enhancement factors at target compressive strains are also very close to those at target tensile strains.

In order to facilitate effective comparison between the stress strain curves of various S690 steel materials under monotonic and cyclic actions, the true stress engineering strain ( $\sigma_t - \varepsilon$ ) hysteretic curves of Test Series A and B are converted into normalized true stress ratio engineering strain ( $\beta_t - \varepsilon$ ) curves, as shown in Figure 20. The backbone curve describing the overall cyclic deformation characteristic of the S690 steel materials is also plotted in the figure. More interestingly, the true stress ratio engineering strain curves obtained from monotonic tensile tests given in Figure 8 are plotted onto Figure 20 for direct comparison. It is shown that the

monotonic curve is very different from the hysteretic curves as well as from the backbone curve. Hence, this comparison quantifies substantial differences in structural responses for the S690 steel materials under monotonic and cyclic tests. Moreover, both hysteretic engineering stress-strain ( $\sigma - \epsilon$ ) curves and hysteretic true stress engineering strain ( $\sigma_t - \epsilon$ ) curves of the S690 steel materials under cyclic loads are obtained, and they are readily applicable for subsequent numerical analyses on the S690 steel materials under seismic loading.

#### 4. Conclusions

Ductility requirements on steel materials are conventionally derived from monotonic tests, and they represent important criteria in selecting suitable steel materials for structural applications. In general, there is no additional requirements stipulated for qualifying these steel materials to be used in seismic resistant structures. As the structural behaviour of steel materials under cyclic loads is rather different from those under monotonic loads, it is important to establish requirements based on realistic cyclic tests on steel materials.

A detailed experimental investigation into structural behaviour of S690 steel materials under both monotonic and cyclic actions has been described in this paper. A total of 6 monotonic tensile tests were conducted to establish basic mechanical properties while 36 cyclic tests were conducted to investigate the hysteretic behaviour under various target strains and loading frequencies. It should be noted that in these cyclic tests, four different target strains, namely,  $\epsilon_m = \pm 2.5\%$ ,  $\pm 5.0\%$ ,  $\pm 7.5\%$  and  $\pm 10\%$ , were specified, and four different loading frequencies, namely,  $f = 0.1, 0.5, 1.0$  and  $2.0$  Hz were employed.

Based on the test results of the presented experimental investigation, it is found that:

- Based on the test results obtained from monotonic tensile tests, all the coupons of S690 steel plates were found to be able to satisfy current ductility requirements stipulated in EN 1993-1-1 and EN 1993-1-12.
- 28 out of 36 specimens were able to complete 20 cycles in the proposed cyclic tests with target strains  $\epsilon_m$  at  $\pm 2.5\%$ ,  $\pm 5.0\%$ ,  $\pm 7.5\%$  and  $\pm 10.0\%$  under various loading frequencies

$f = 0.1, 0.5, 1.0$  and  $2.0$  Hz. However, 8 coupons did fracture at the 20<sup>th</sup> cycle when the target strains were  $\pm 10.0$  % irrespective of the loading frequencies.

- As there is significant reduction (or enlargement) in the cross-sectional areas of the coupon under tension (or compression), it is important to use instantaneous diameters to evaluate true stresses respectively.
- By comparing the normalized true stress ratio engineering strain ( $\beta_t - \epsilon$ ) curves obtained from monotonic and cyclic tests, it is evident that they behave very differently at an engineering strain at 5% or above.

Based on these test data and their analyses, a constitutive model for the S690 steel materials under both monotonic and cyclic loadings will be developed for effective use in seismic resistant structures. The proposed constitutive model will be reported separately.

## **Acknowledgement**

The authors are grateful to the financial support provided by the Research Grant Council of the Government of Hong Kong SAR (Project Nos. PolyU 5143/13E and 152194/15E). The project leading to the publication of this paper is also partially funded by the Research Committee (Project Nos. RTK3 and RUQV) and the Chinese National Engineering Research Centre for Steel Construction (Hong Kong Branch) (Project No. 1-BBY3 & 6) of the Hong Kong Polytechnic University. The research studentships of the second and the fifth authors provided by the Hong Kong Polytechnic University are acknowledged. Special thanks go to the Nanjin Iron and Steel Company Ltd. in Nanjin, the Pristine Steel Fabrication Company Ltd. in Dongguang, and the Industrial Centre of the Hong Kong Polytechnic University.

All structural tests on high strength S690 steel materials were carried out at the Structural Engineering Research Laboratory of the Department of Civil and Environmental Engineering at the Hong Kong Polytechnic University, and supports from the technicians are gratefully acknowledged.

## **REFERENCES**

- ANSI-AISC 341-16 (2016). Seismic Provisions for Structural Steel Buildings, Standard, American Institute of Steel Construction, Chicago, Illinois, USA.
- BS 3518-3 (1963). Method of fatigue testing – Part 3: Direct stress fatigue tests. British Standards Institution.

- BS EN ISO 6892-1 (2009). Metallic materials – Tensile testing: Part 1: Method of test at ambient temperature, British Standards Institution.
- BS EN 1993-1-1 (2005). Design of Steel Structures – Part 1-1: General rules and rules for buildings. British Standards Institution.
- BS EN 1993-1-12 (2007). Design of Steel Structures – Part 1-12: Additional rules for the extension of EN 1993 up to steel grades S700. British Standards Institution.
- Chen Y., Sun W. and Chan T.M. (2013). “Effect of loading protocols on the hysteresis behavior of hot-rolled structural steel with yield strength up to 420 MPa.” *Advances in Structural Engineering*. 16(4), 707-719.
- Deierlein G. G., Reinhorn, A. M., and Willford, M. R. (2010). NEHRP Seismic Design Technical Brief No.4 – Nonlinear Structural Analysis for Seismic Design – A Guide for Practicing Engineers. National Institute of Standards and Technology (NIST), Gaithersburg, U.S.A.
- ECCS (1986). Seismic design. Recommended testing procedure for assessing the behaviour of structural steel elements under cyclic loads. Tech. comm. 1 - Structural safety and loadings. TWG 1.3 Rep. no. 45.
- Fournier, B., Sauzay M., Caës, C., Noblecourt M., and Mottot, M. (2006a). “Analysis of the hysteresis loops of a martensitic steel – Part I: Study of the influence of strain amplitude and temperature under pure fatigue loadings using an enhanced stress partitioning method.” *Materials Science and Engineering A*. 437, 183-196.
- Fournier, B., Sauzay M., Caës, C., Mottot, M., Noblecourt M., and Pineau, A. (2006b). “Analysis of the hysteresis loops of a martensitic steel – Part II: Study of the influence of creep and stress relaxation holding times on cyclic behaviour.” *Materials Science and Engineering A*. 437, 197-211.
- FEMA-461 (2007). Interim testing protocols for determining the seismic performance characteristics of structural and non-structural components.
- GB/T 15248 (1994). Metallic Materials – Constant Amplitude Strain Controlled Axial Fatigue – Method of Test. Standard Press of China, Beijing, China. (In Chinese)
- Dieter G.E. (1961). *Mechanical Metallurgy*. New York, McGraw-Hill, U.S.A.
- Ho H.C., Liu X., Chan T.M. and Chung K.F. (2016). “Hysteretic behavior of Q275 and Q690 structural steel materials”, *Proceedings of the 14th East Asia-Pacific Conference on Structural Engineering and Construction (EASEC-14)*, Ho Chi Minh City, Vietnam, 6–8 January 2016.
- Ho H.C., Liu X., Xiao M. and Chung K.F. (2016). Experimental investigation into hysteretic behaviour of high strength S690 steel under different targeted strains. *Proceeding of the Eighth International Conference on Steel and Aluminium Structures*, Hong Kong, December 2016, 2016, p1485-1496. (Paper No.: 101)
- Ho H.C., Xiao M., Liu X., and Chung K.F. (2017). Tensile tests on high strength steel materials using high precision measurement. *Proceeding of 14th East Asia-Pacific Conference on Structural Engineering and Construction (EASEC-15)*, Xi'an, October 2017. (Paper No.: A1404)
- ISO 12106 (2003). Metallic materials –Fatigue testing – Axial-strain-controlled method.
- Khan S., Wilde F., Beckmann F., and Mosler J. (2012). “Low cycle fatigue mechanism of the lightweight alloy Al2024.” *International Journal of Fatigue*. 38, 92-99.
- Kia S. M. and Yahyai M. (2004). “Relationship between local and global ductility demand in steel moment resisting frames.” *Proc., The 13<sup>th</sup> World Conference on Earthquake Engineering*, Vancouver, B.C., Canada, August 1-6.
- Krawinkler H. and Nassar A. (1990). “Strength and ductility demands for SDOF and MDOF systems subjected to whittier narrows earthquake ground motions.” *Proc., SMIP 1990*



Seminar on Seismological and Engineering Implications of Recent Strong-Motion Data, Sacramento, California, June 8.

- Krawinkler H., Medina R., and Alavi B. (2003). "Seismic drift and ductility demands and their dependence on ground motion." *Engineering Structures*, 25, 637-653.
- Li Y. Pan X. and Wang G. (2013). "Low cycle fatigue and ratcheting properties of steel 40Cr under stress controlled tests." *International Journal of Fatigue*. 55, 74-80.
- Mergos P. E. and Beyer K. (2014). "Loading Protocols for European regions of low to moderate seismicity." *Bulletin of Earthquake Engineering*. 12, 2507-2530.
- Nip, K. H., Gardner, L., Davies, C. M., and Elghazouli, A. Y. (2010). "Extremely low cycle fatigue tests on structural carbon steel and stainless steel." *Journal of Constructional Steel Research*, 66, 96-110.
- Pacific Earthquake Engineering Research Center. (2010). "Guidelines for Performance-Based Seismic Design of Tall Buildings." College of Engineering, University of California, Berkeley, U.S.A.
- Shafei B. and Zareian F. (2008). "Development of a quasi-static loading protocol for displacement-sensitive non-structural building components." *Proc., The 14<sup>th</sup> World Conference on Earthquake Engineering*, Beijing, China, October 12-17.
- Tsitos A, Elghazouli AY. (2017). Evaluation of loading protocols for assessing local seismic demands in steel buildings designed to EC8, 16th World Conference on Earthquake Engineering, Pages: Paper No 1559-Paper No 1559.
- Wang, Y. B., Li, G. Q., Sun, X., Chen, S., & Hai, L. T. (2017). Evaluation and prediction of cyclic response of Q690D steel. *Proceedings of the Institution of Civil Engineers-Structures and Buildings*, 1-16.
- Zhou F., Chen Y., and Wu Q. (2015). "Dependence of the cyclic response of structural steel on loading history under large inelastic strains." *Journal of Constructional Steel Research*, 104, 64-73.

**Table 1. Max % of chemical compositions**

Steel Grade		C	Si	Mn	P	S	N	B	Cr	Cu	Mo	Nb	Ni	Ti	V	Zr
S690	BS EN 10025-6	0.22	0.86	1.8	0.025	0.012	0.016	0.006	1.6	0.55	0.74	0.07	2.1	0.07	0.14	0.17
	Test	0.137	0.22	1.377	0.010	0.0012	0.004	-	0.33	0.485	0.24	0.026	0.037	0.012	-	-

**Table 2. Test programme of monotonic tensile tests**

Test	Thickness of original plates (mm)	Type of coupons	Diameter, $d$ (mm)	Gauge length, $L_0$ (mm)	Total length, $L$ (mm)
T690-A1 T690-A2 T690-A3	16	cylindrical	6	30	130
T690-B1 T690-B2 T690-B3	25	cylindrical	6	30	130

**Table 3. Loading rates for monotonic tensile tests**

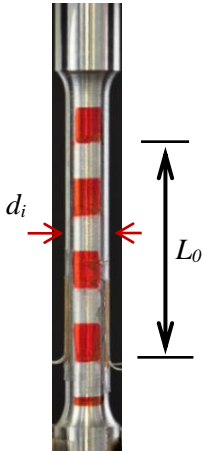
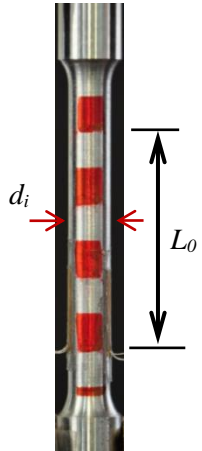
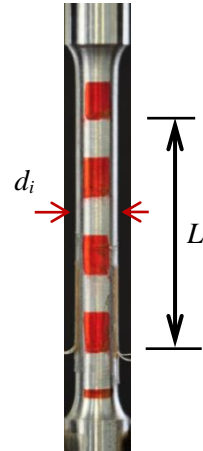
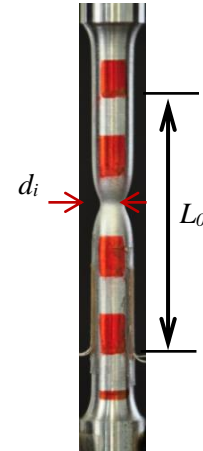
Stage	Purpose	Loading rates	
		BS EN ISO 6892-1	Test
1	Determination of E	360 ~ 3600 N/mm <sup>2</sup> /min	10 ~ 50 N/mm <sup>2</sup> /min
2	Determination of $f_y$	0.015 ± 0.003 mm/mm/min	0.0002 ~ 0.0015 mm/mm/min
3	Determination of $f_u$ and $\epsilon_L$	0.15 ± 0.03 mm/mm/min	0.002 ~ 0.012 mm/mm/min

**Table 4. Measured mechanical properties of S690 steel materials**

Thickness of original plate (mm)	Specimen	Diameter (mm)	E (kN/mm <sup>2</sup> )	$f_y$ (N/mm <sup>2</sup> )	$f_u$ (N/mm <sup>2</sup> )	$f_u / f_y$	$\epsilon_u$ (%)	$\epsilon_L$ (%)
16	T690-A1	5.98	212.4	798.4	850.9	1.07	7.1	18.0
	T690-A2	6.00	209.0	782.0	848.7	1.09	7.1	17.5
	T690 -A3	5.98	216.2	808.8	850.5	1.05	6.1	17.7
average value			212.5	796.4	850.0	1.07	6.8	17.7
CV			0.017	0.017	0.001	0.019	0.083	0.014

Thickness of original plate (mm)	Specimen	Diameter (mm)	E (kN/mm <sup>2</sup> )	$f_y$ (N/mm <sup>2</sup> )	$f_u$ (N/mm <sup>2</sup> )	$f_u / f_y$	$\epsilon_u$ (%)	$\epsilon_L$ (%)
25	T690-B1	6.02	215.7	734.8	773.8	1.05	6.2	17.5
	T690-B2	6.02	217.5	734.9	773.0	1.05	6.0	17.8
	T690-B3	5.98	222.7	748.8	781.7	1.04	5.5	17.3
average value			218.6	739.5	776.2	1.05	5.9	17.5
CV			0.014	0.011	0.006	0.005	0.050	0.012

**Table 5. Typical example to determine average strains by the use of digital photos**

	Initial Condition	Strain corresponding to yield condition	Strain corresponding to ultimate condition	Strain corresponding to fracture condition
Digital Photos				
$L_o$ (pixel)	1080	1085	1152	1273
$L_o$ (mm)	30.00	30.14	32.00	35.36
Strain (%)	0.00	0.46	6.70	17.90

**Table 6. Strains of various segments within the gauge length**

Deformation	Strain (%) of each segment						Average strain (%) of Segment No. 1 to 6	Strain measured by strain gauge (%)
	No. 1	No. 2	No. 3	No. 4	No. 5	No. 6		
Yield condition	0.00	0.70	0.00	0.75	0.00	1.30	0.46	0.36
Ultimate condition	6.30	6.70	6.80	6.82	6.70	6.86	6.70	6.72
Fracture condition	5.67	5.75	8.51	69.0	9.04	9.14	17.9	-

Note: The overall gauge length is 30 mm, and there are a total of 6 segments. Hence, the length of each segment is 5.0 mm.

**Table 7. Strain amplitudes at various load cycles for  $\epsilon_m = \pm 10.0\%$  and  $f = 0.1\text{ Hz}$** 

Step	Load cycle	Strain, $\epsilon_i$ (%)	Maximum straining rate (% / s)
1	1 ~ 2	$\epsilon_1, \epsilon_2 = \pm 0.48$	0.30
2	3 ~ 4	$\epsilon_3, \epsilon_4 = \pm 0.68$	0.43
3	5 ~ 6	$\epsilon_5, \epsilon_6 = \pm 0.95$	0.60
4	7 ~ 8	$\epsilon_7, \epsilon_8 = \pm 1.33$	0.83
5	9 ~ 10	$\epsilon_9, \epsilon_{10} = \pm 1.86$	1.17
6	11 ~ 12	$\epsilon_{11}, \epsilon_{12} = \pm 2.60$	1.64
7	13 ~ 14	$\epsilon_{13}, \epsilon_{14} = \pm 3.64$	2.29
8	15 ~ 16	$\epsilon_{15}, \epsilon_{16} = \pm 5.10$	3.21
9	17 ~ 18	$\epsilon_{17}, \epsilon_{18} = \pm 7.14$	4.49
10	19 ~ 20	$\epsilon_{19}, \epsilon_{20} = \pm 10.0$	6.28

**Table 8. Test programme of cyclic tests**

Test Series A1 and A2

Thickness of original plates (mm)	Targeted strain, $\epsilon_m$ Frequency, f (Hz)		$\pm 2.5\%$	$\pm 5.0\%$	$\pm 7.5\%$	$\pm 10.0\%$
16	0.1		2	2	2	2
	0.5		-	2	-	2
	1.0		-	2	-	2
	2.0		-	2	-	2

Test Series B1 and B2

Thickness of original plates (mm)	Targeted strain, $\epsilon_m$ Frequency, f (Hz)		$\pm 2.5\%$	$\pm 5.0\%$	$\pm 7.5\%$	$\pm 10.0\%$
25	0.1		-	2	-	2
	0.5		-	2	-	2
	1.0		-	2	-	2
	2.0		-	2	-	2

**Table 9. Engineering stress-strain hysteretic properties of S690 steel materials**

Specimen	Targeted strain, $\varepsilon_m$ (%)	Loading frequency (Hz)	Maximum straining rate (%/s)	Number of completed cycles	0.2% proof strength, $f_{0.2,c}$ (N/mm <sup>2</sup> )		Strength at targeted strain, $f_{\varepsilon m,c}$ (N/mm <sup>2</sup> )		Strength enhancement factor, $\eta$	
					T	C	T	C	T	C
Test Series A1										
AA-025a	$\pm 2.5$	0.1	1.57	20	+807	-824	+857	-952	1.06	1.15
AA-025b				20	+805	-810	+849	-938	1.05	1.16
AA-050a	$\pm 5.0$	0.1	3.14	20	+814	-837	+818	-984	1.00	1.18
AA-050b				20	+806	-832	+809	-964	1.00	1.16
AA-075a	$\pm 7.5$	0.1	4.71	20	+825	-847	+786	-1025	0.95	1.21
AA-075b				20	+813	-837	+756	-991	0.93	1.18
AA-100a	$\pm 10.0$	0.1	6.28	19	+834	-839	+709	-1045	0.85	1.25
AA-100b				19	+839	-848	+718	-1056	0.86	1.25
Test Series A2										
AA-050a	$\pm 5.0$	0.1	3.14	20	+814	-837	+818	-984	1.00	1.18
AA-050b				20	+806	-832	+809	-964	1.00	1.16
AB-050a		0.5	15.71	20	+808	-834	+795	-987	0.98	1.18
AB-050b				20	+802	-851	+781	-994	0.96	1.17
AC-050a		1.0	31.42	20	+813	-811	+793	-939	0.98	1.16
AC-050b				20	+817	-822	+788	-960	0.96	1.17
AD-050a		2.0	62.83	20	+812	-819	+783	-937	0.96	1.15
AD-050b				20	+816	-831	+791	-957	0.97	1.15
AA-100a	$\pm 10.0$	0.1	6.28	19	+834	-839	+709	-1045	0.85	1.25
AA-100b				19	+839	-848	+718	-1056	0.86	1.25
AB-100a		0.5	31.42	19	+805	-867	+650	-1095	0.81	1.26
AB-100b				19	+798	-875	+648	-1103	0.81	1.26
AC-100a		1.0	62.83	19	+820	-833	+697	-1059	0.85	1.27
AC-100b				19	+825	-834	+702	-1054	0.85	1.26
AD-100a		2.0	125.66	19	+830	-843	+723	-1060	0.87	1.26
AD-100b				19	+827	-835	+697	-1064	0.84	1.27

Note: T denotes tension  
C denotes compression

Specimen	Targeted strain, $\varepsilon_m$ (%)	Loading frequency (Hz)	Maximum straining rate (%/s)	Number of completed cycles	0.2% proof strength, $f_{0.2,c}$ (N/mm <sup>2</sup> )		Strength at targeted strain, $f_{\varepsilon m,c}$ (N/mm <sup>2</sup> )		Strength enhancement factor, $\eta$		
					T	C	T	C	T	C	
Test Series B1											
BA-025a BA-025b	-	-	-	-	-		-		-		
BA-050a BA-050b	± 5.0	0.1	3.14	20 20	+751 +743	-753 -756	+744 +740	-881 -888	0.99 1.00	1.17 1.17	
BA-075a BA-075b	-	-	-	-	-		-		-		
BA-100a BA-100b	± 10.0	0.1	6.28	20 20	+753 +760	-763 -770	+674 +685	-993 -957	0.90 0.90	1.30 1.24	
Test Series B2											
BA-050a BA-050b	± 5.0	0.1	3.14	20 20	+751 +743	-753 -756	+744 +740	-881 -888	0.99 1.00	1.17 1.17	
BB-050a BB-050b		0.5	15.71	20 20	+753 +762	-775 -782	+720 +756	-891 -899	0.96 0.99	1.15 1.15	
BC-050a BC-050b		1.0	31.42	20 20	+766 +749	-750 -696	+753 +692	-866 -814	0.98 0.92	1.15 1.17	
BD-050a BD-050b		2.0	62.83	20 20	+754 +767	-783 -798	+714 +734	-861 -885	0.95 0.96	1.10 1.11	
BA-100a BA-100b		± 10.0	0.1	6.28	20 20	+753 +760	-763 -770	+674 +685	-993 -957	0.90 0.90	1.30 1.24
BB-100a BB-100b			0.5	31.42	20 20	+752 +769	-757 -803	+659 +642	-939 -970	0.88 0.83	1.24 1.21
BC-100a BC-100b	1.0		62.83	20 20	+739 +774	-759 -785	+632 +624	-992 -939	0.86 0.81	1.31 1.20	
BD-100a BD-100b	2.0		125.66	20 20	+748 +762	-759 -778	+659 +648	-922 -918	0.88 0.85	1.21 1.18	

Note: T denotes tension  
C denotes compression

**Table 10. True stress-engineering strain hysteretic properties of S690 steel materials**

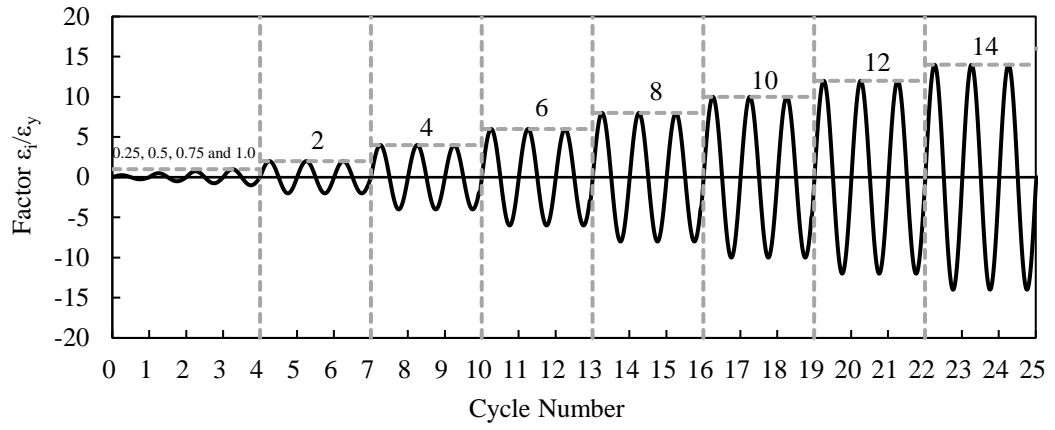
Specimen	Targeted strain, $\varepsilon_m$ (%)	Loading frequency (Hz)	Maximum straining rate (%/s)	Number of completed cycles	0.2% proof strength, $f_{0.2,c}$ (N/mm <sup>2</sup> )		Strength at targeted strain, $f_{\varepsilon m,c}$ (N/mm <sup>2</sup> )		Strength enhancement factor, $\eta$	
					T	C	T	C	T	C
Test Series A1										
AA-025a	$\pm 2.5$	0.1	1.57	20	+816	-817	+913	-932	1.11	1.14
AA-025b				20	+813	-804	+899	-919	1.11	1.14
AA-050a	$\pm 5.0$	0.1	3.14	20	+823	-846	+969	-981	1.18	1.16
AA-050b				20	+816	-842	+963	-965	1.18	1.15
AA-075a	$\pm 7.5$	0.1	4.71	20	+834	-857	+1107	-1080	1.33	1.26
AA-075b				20	+822	-846	+1075	-1044	1.31	1.23
AA-100a	$\pm 10.0$	0.1	6.28	19	+856	-849	+1331	-1285	1.55	1.51
AA-100b				19	+861	-857	+1347	-1297	1.56	1.51
Test Series A2										
AA-050a	$\pm 5.0$	0.1	3.14	20	+823	-846	+969	-981	1.18	1.16
AA-050b				20	+816	-842	+963	-965	1.18	1.15
AB-050a		0.5	15.71	20	+817	-827	+974	-1005	1.19	1.17
AB-050b				20	+811	-844	+946	-1014	1.21	1.20
AC-050a		1.0	31.42	20	+822	-820	+972	-959	1.18	1.17
AC-050b				20	+826	-831	+963	-978	1.17	1.18
AD-050a		2.0	62.83	20	+827	-819	+958	-956	1.16	1.17
AD-050b				20	+832	-827	+968	-976	1.16	1.18
AA-100a	$\pm 10.0$	0.1	6.28	19	+856	-849	+1331	-1285	1.55	1.51
AA-100b				19	+861	-857	+1347	-1297	1.56	1.51
AB-100a		0.5	31.42	19	+813	-867	+1213	-1330	1.49	1.53
AB-100b				19	+821	-875	+1207	-1344	1.47	1.54
AC-100a		1.0	62.83	19	+836	-832	+1288	-1287	1.54	1.55
AC-100b				19	+841	-833	+1299	-1273	1.54	1.53
AD-100a		2.0	125.66	19	+847	-839	+1357	-1300	1.60	1.55
AD-100b				19	+843	-831	+1308	-1304	1.55	1.57

Note: T denotes tension  
C denotes compression

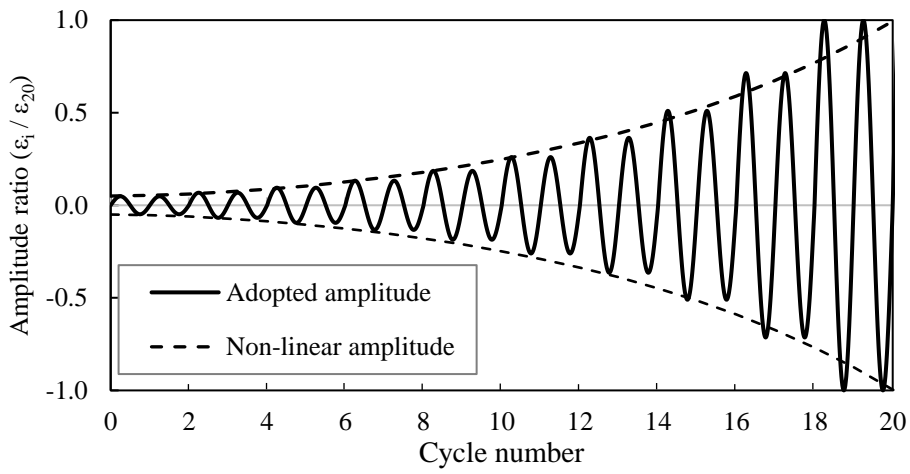


Specimen	Targeted strain, $\varepsilon_m$ (%)	Loading frequency (Hz)	Maximum straining rate (%/s)	Number of completed cycles	0.2% proof strength, $f_{0.2,c}$ (N/mm <sup>2</sup> )		Strength at targeted strain, $f_{\varepsilon m,c}$ (N/mm <sup>2</sup> )		Strength enhancement factor, $\eta$		
					T	C	T	C	T	C	
Test Series B1											
BA-025a BA-025b	-	-	-	-	-		-		-		
BA-050a BA-050b	± 5.0	0.1	3.14	20 20	+775 +752	-786 -749	+923 +924	-927 -914	1.19 1.23	1.18 1.22	
BA-075a BA-075b	-	-	-	-	-		-		-		
BA-100a BA-100b	± 10.0	0.1	6.28	20 20	+761 +768	-755 -764	+1212 +1199	-1203 -1199	1.59 1.60	1.59 1.57	
Test Series B2											
BA-050a BA-050b	± 5.0	0.1	3.14	20 20	+775 +752	-786 -749	+923 +924	-927 -914	1.19 1.23	1.18 1.22	
BB-050a BB-050b		0.5	15.71	20 20	+761 +769	-775 -775	+918 +917	-938 -926	1.21 1.19	1.21 1.19	
BC-050a BC-050b				1.0	31.42	20 20	+783 +758	-770 -690	+945 +862	-889 -842	1.21 1.14
BD-050a BD-050b		2.0	62.83			20 20	+765 +775	-780 -792	+879 +920	-890 -907	1.17 1.19
BA-100a BA-100b				± 10.0	0.1	6.28	20 20	+761 +768	-755 -764	+1212 +1199	-1203 -1199
BB-100a BB-100b		0.5	31.42		20 20	+766 +778	-749 -800	+1216 +1216	-1163 -1189	1.59 1.56	1.55 1.49
BC-100a BC-100b	1.0				62.83	20 20	+755 +783	-748 -779	+1199 +1256	-1139 -1157	1.59 1.60
BD-100a BD-100b		2.0	125.66			20 20	+755 +770	-749 -772	+1240 +1198	-1153 -1129	1.64 1.56

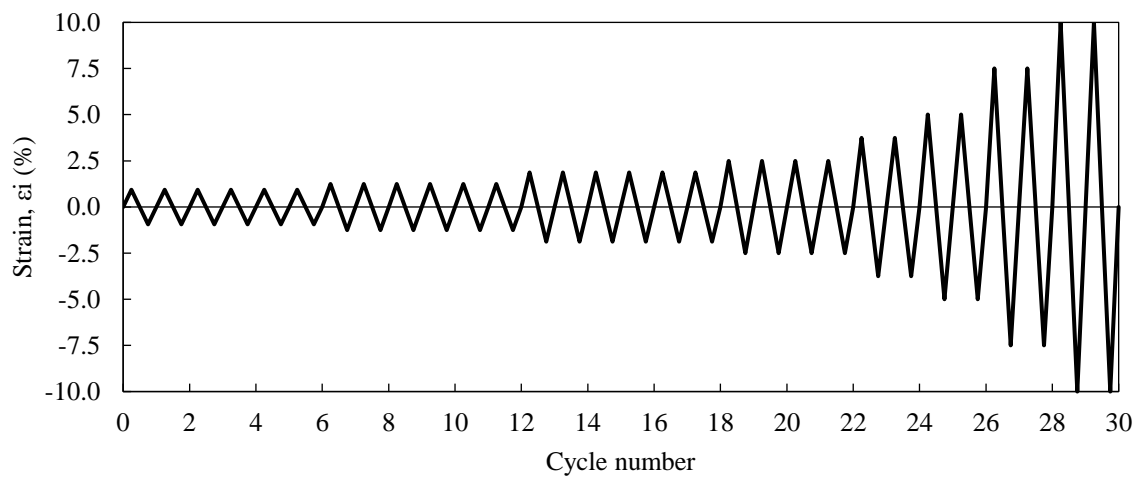
Note: T denotes tension  
C denotes compression



a) Loading protocol to ECCS



b) Loading protocol to FEMA-461



c) Loading protocol to AISC 341

**Figure 1 Comparison among three recommended loading protocols**

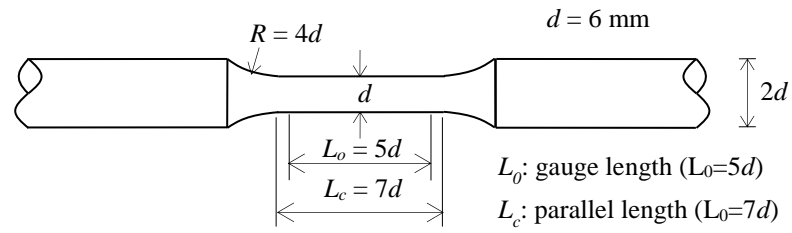


**Figure 2. Geometry and dimensions of test coupons for monotonic tensile tests**

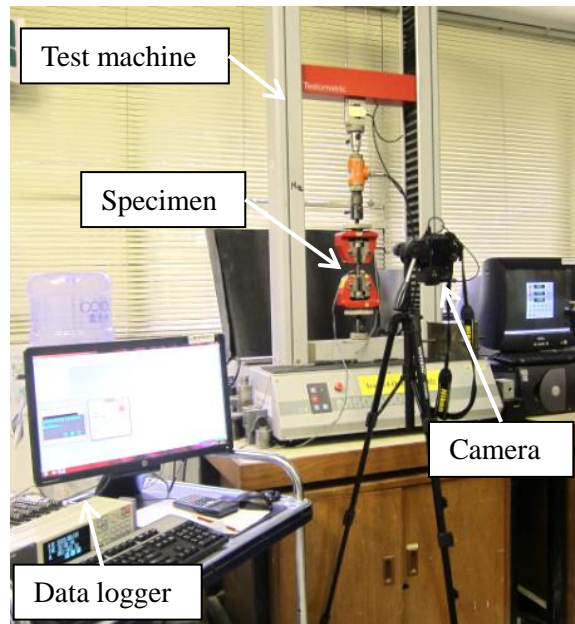


**Figure 3. Set-up and instrumentation for monotonic tensile tests**

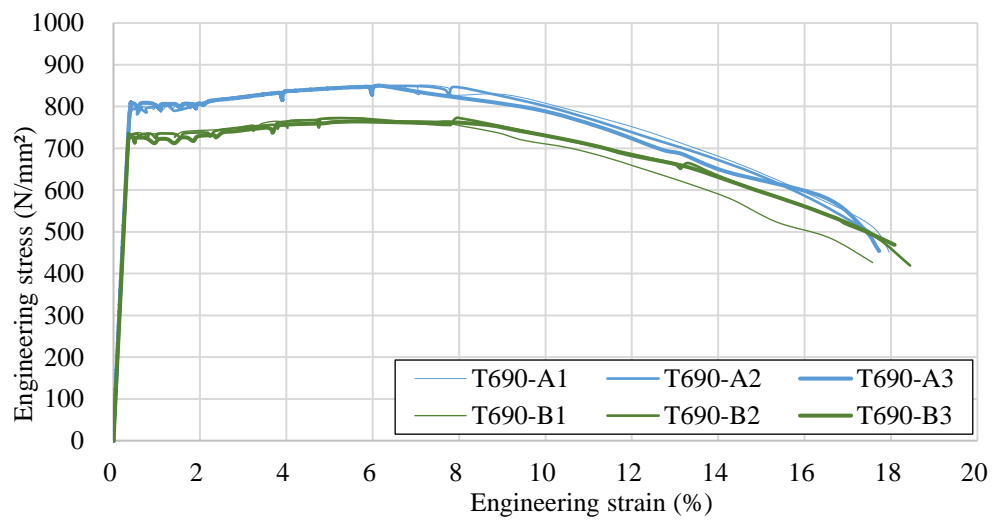
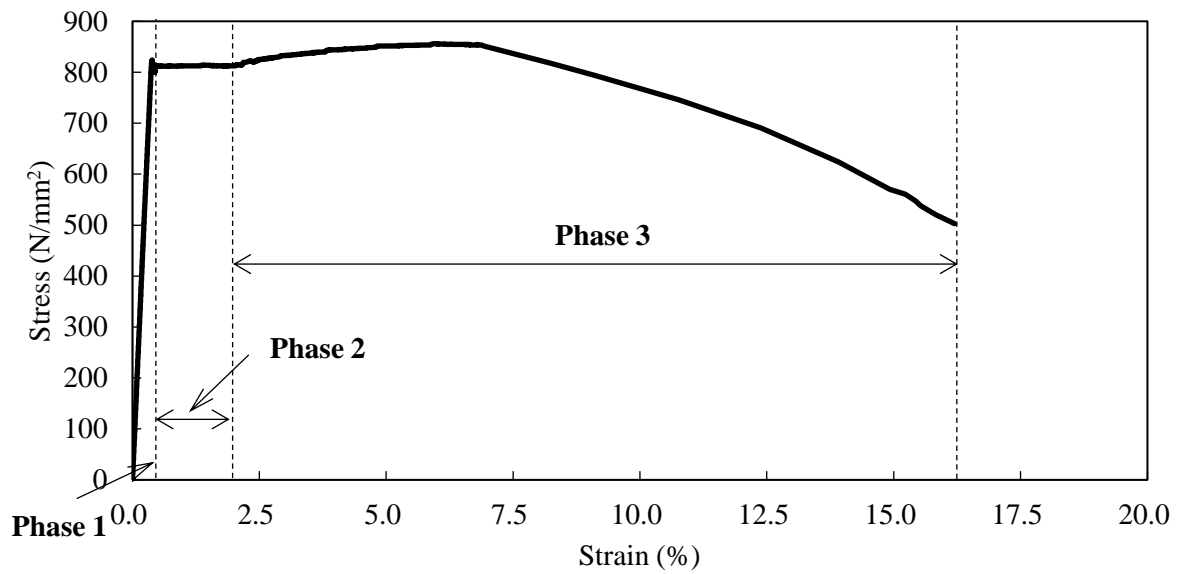
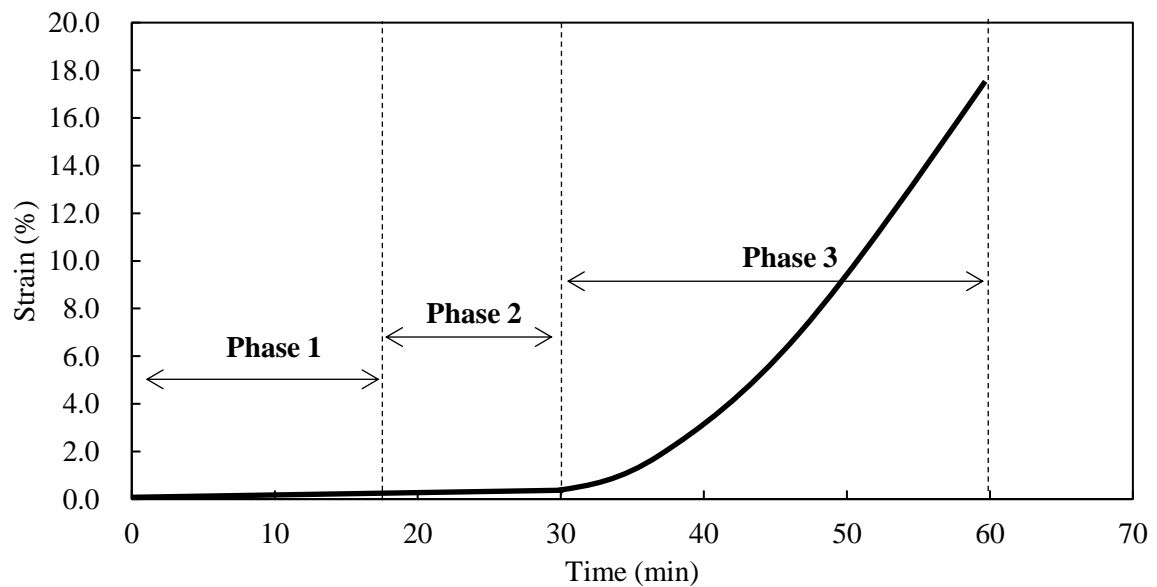


**Figure 4. Engineering stress-strain curves of monotonic tensile tests**



Phase 1: Linear elastic phase for determination of Young's modulus  
 Phase 2: Yield plateau phase for determination of yield strength  
 Phase 3: Non-linear phase for determination of tensile strength

**Figure 5. Typical stress-strain curve of monotonic tensile tests**



Phase 1: Linear elastic phase for determination of Young's modulus  
 Phase 2: Yield plateau phase for determination of yield strength  
 Phase 3: Non-linear phase for determination of tensile strength

**Figure 6. Transient strain history during testing**

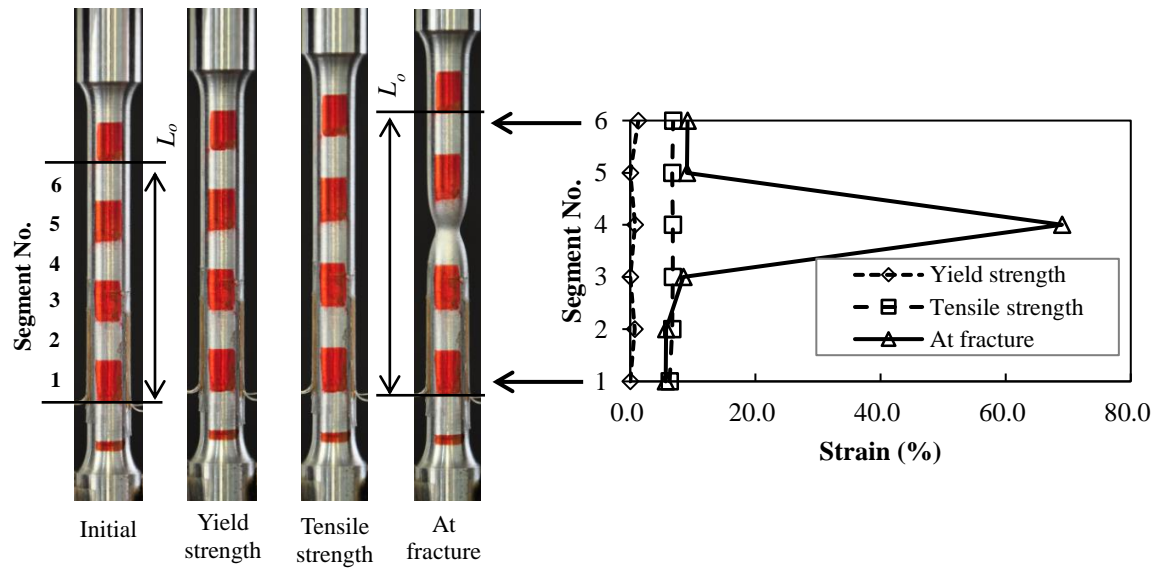


Figure 7. Strain distributions of different segments

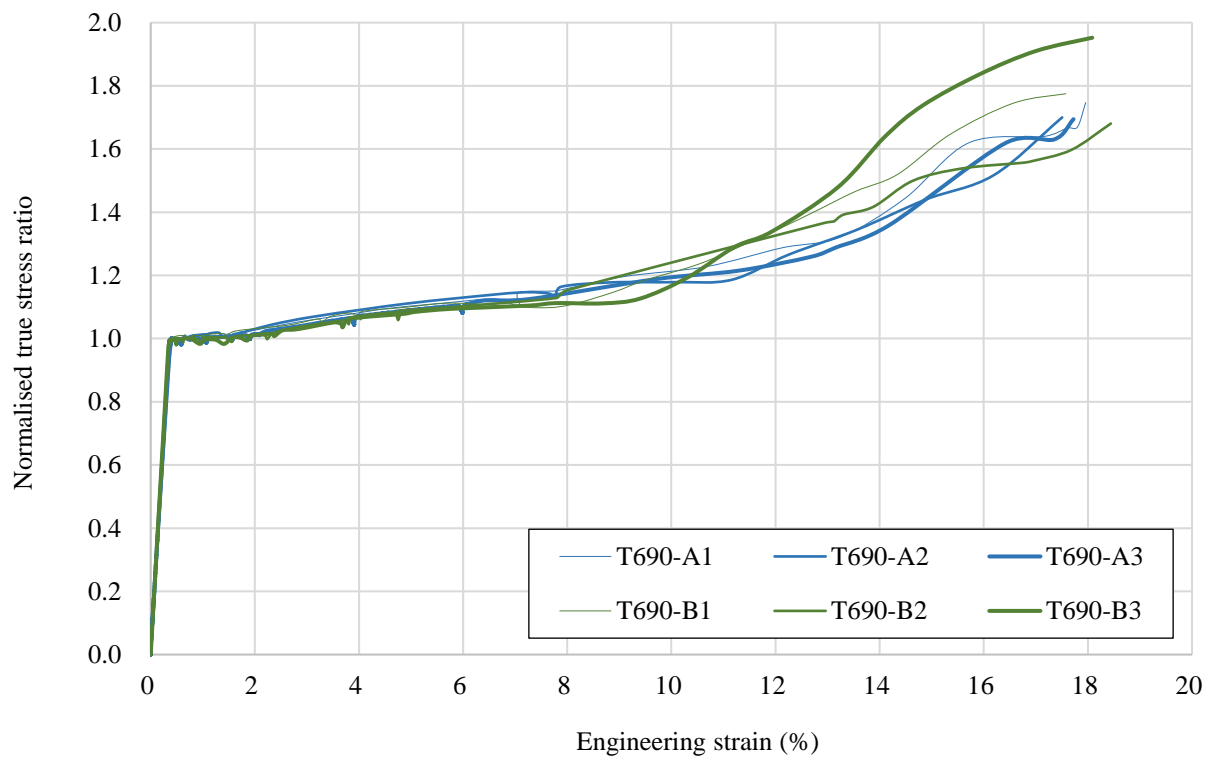
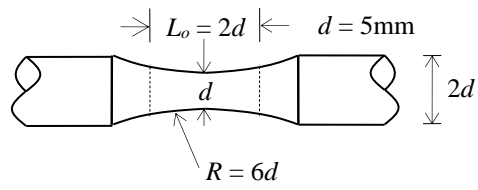


Figure 8. Normalized true stress ratio engineering strain curves of monotonic tensile tests



**Figure 9. Dimensions of funnel-shaped coupons under cyclic tests**



i) overall view



ii) a coupon with an extensometer



iii) a fractured coupon

**Figure 10. Typical set-up of cyclic tests**

## Test Series A1

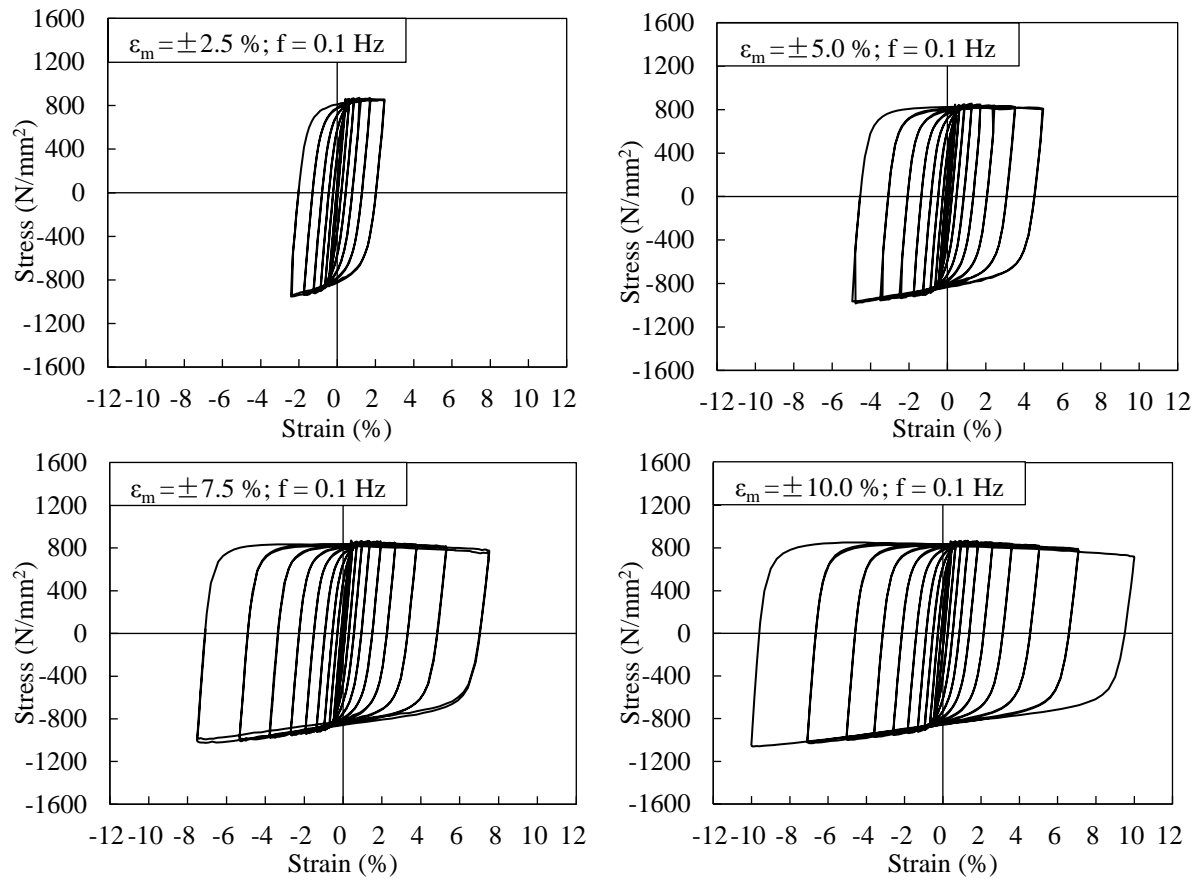


**Figure 11. Engineering hysteretic stress-strain curves at various targeted strains**

# Test Series A1 and A2

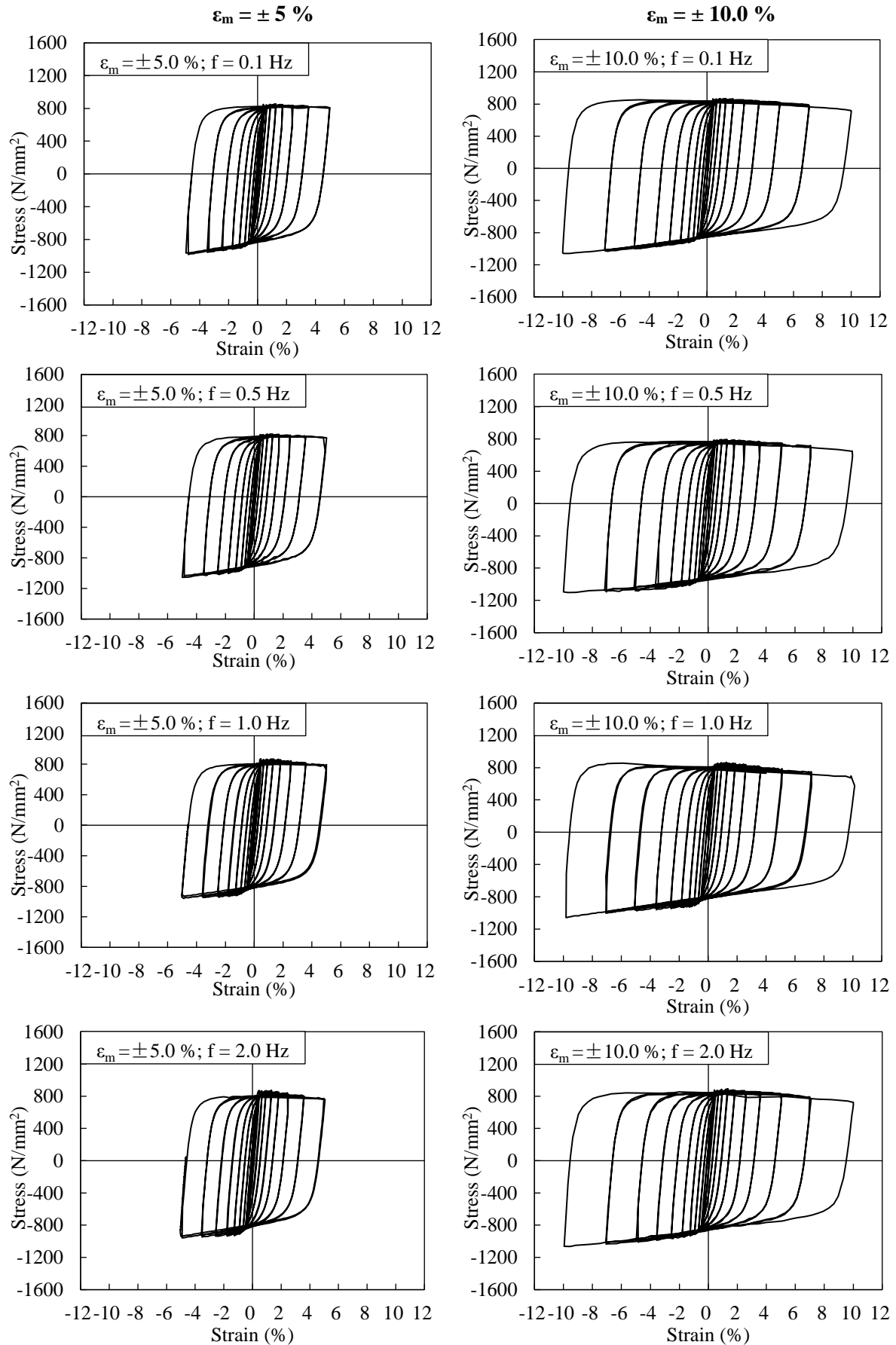


**Figure 12. Engineering hysteretic stress-strain curves under various frequencies**



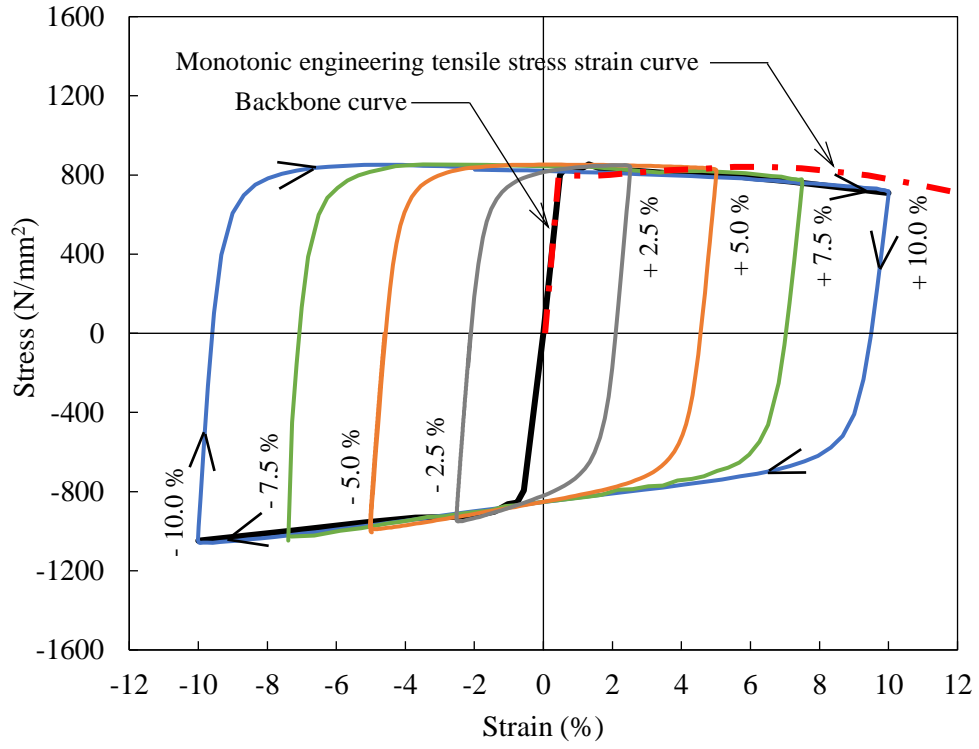


**Figure 13. Engineering hysteretic loops at various targeted strains**

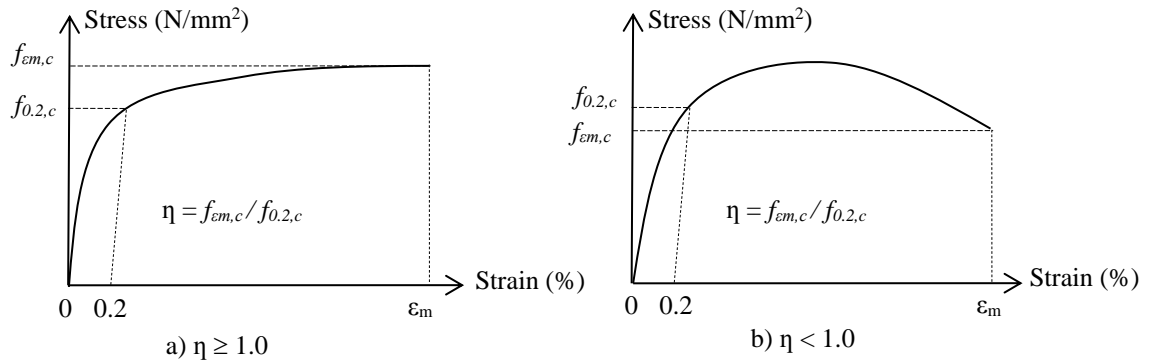


**Figure 14. Definition of strength enhancement factor,  $\eta$**

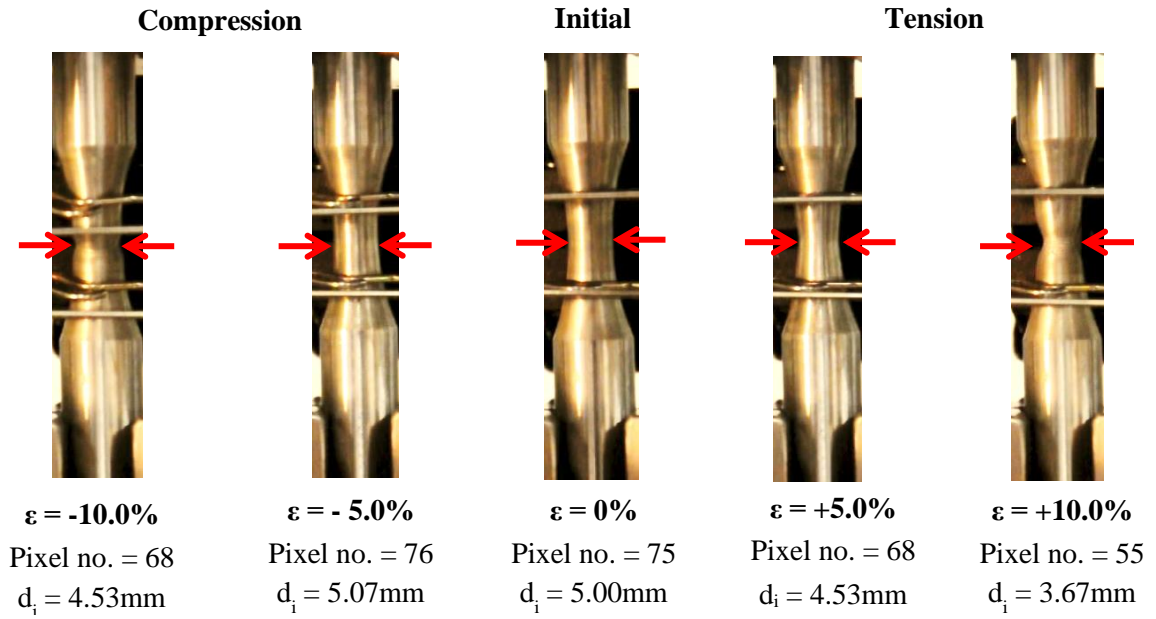


**Figure 15. Instantaneous diameters at various targeted strains**

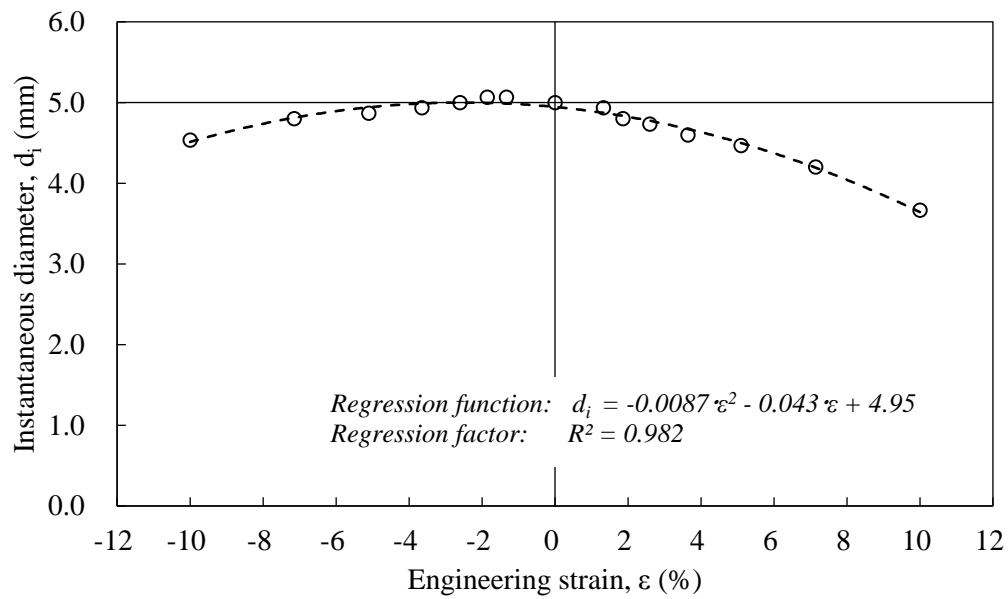


**Figure 16. Instantaneous diameters,  $d_i$ , under various strains**

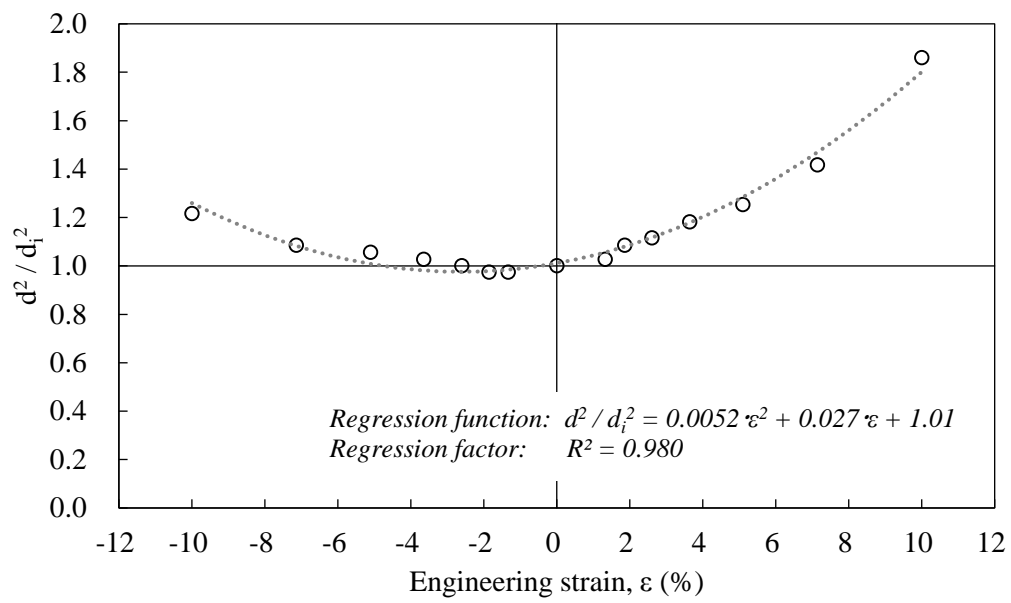


**Figure 17. Values of convention factor to engineering stresses**

# Test Series A1

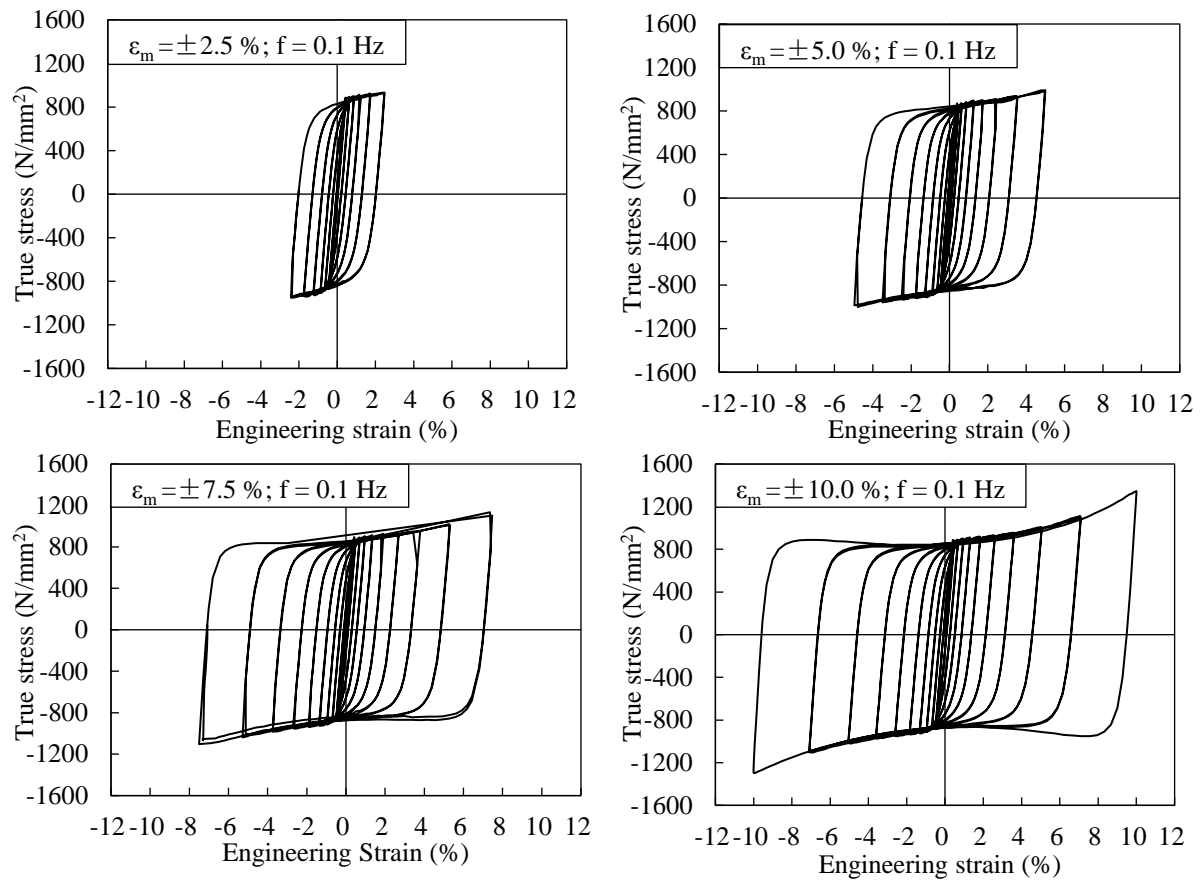


**Figure 18. Hysteretic stress-strain curves at various targeted strains  
-true stress ( $\sigma_t$ ) against engineering strain ( $\epsilon$ )**

# Test Series A1 and A2

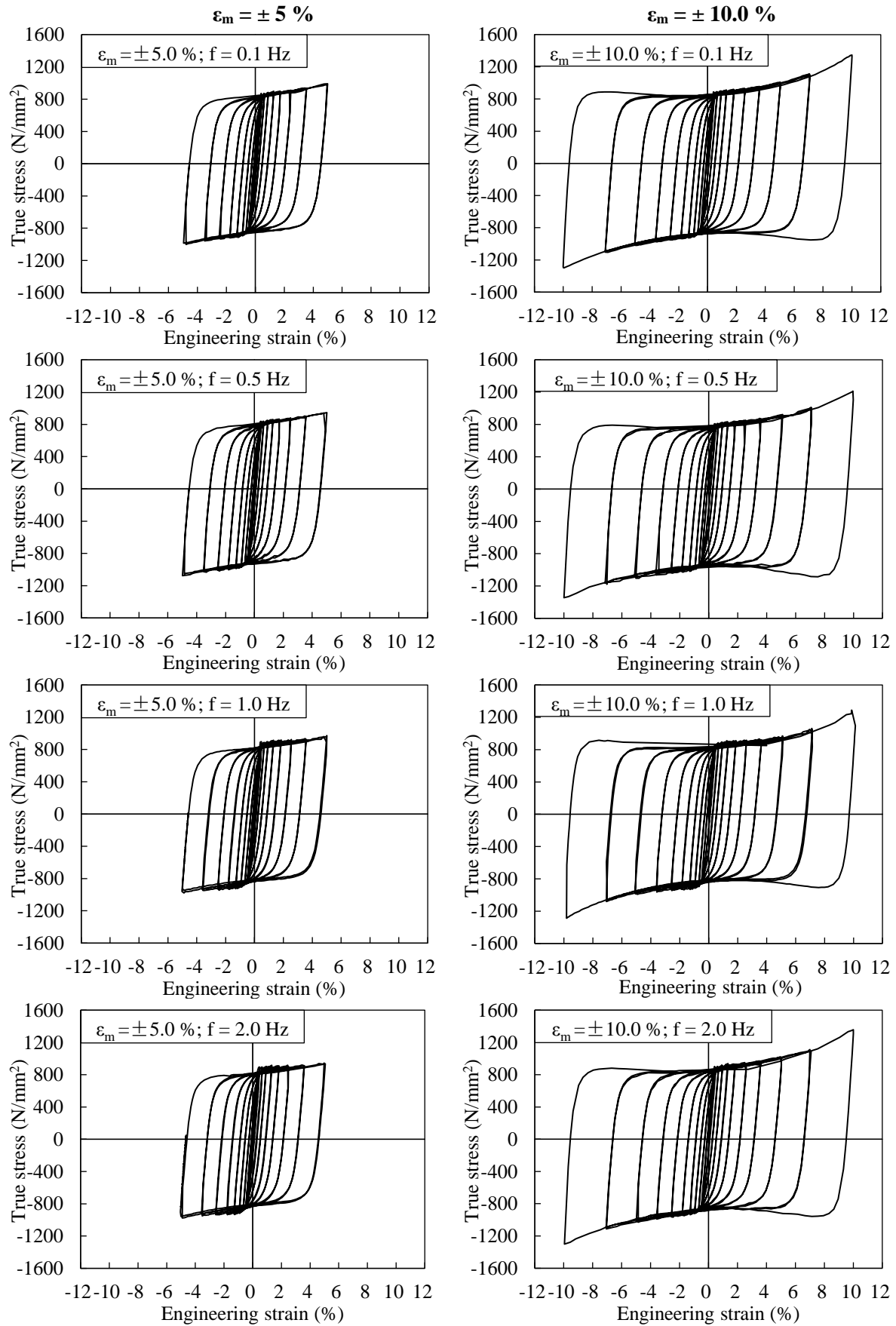


**Figure 19. Hysteretic stress-strain curves under various frequencies**  
**-true stress ( $\sigma_t$ ) against engineering strain ( $\epsilon$ )**

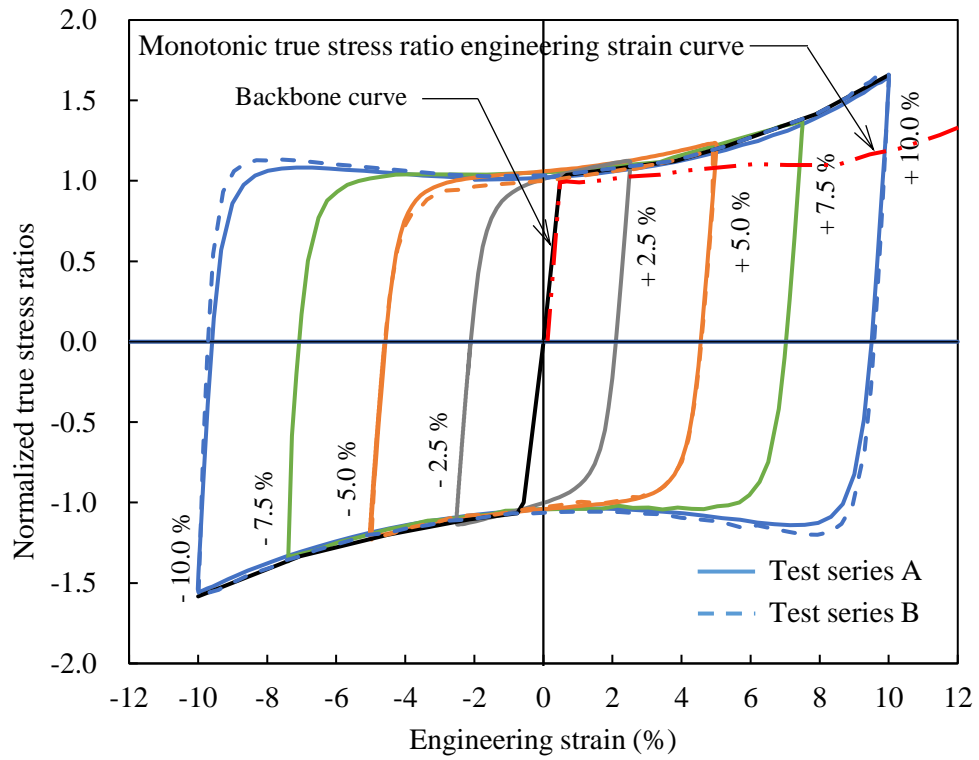


**Figure 20. Hysteretic loops at various targeted strains**